

# Reversible Quantum Interface for Tunable Single-sideband Modulation

J. Cviklinski, J. Ortalo, J. Laurat, A. Bramati, M. Pinard, E. Giacobino\*

*Laboratoire Kastler Brossel, Université Pierre et Marie Curie,  
Ecole Normale Supérieure, CNRS, 4 place Jussieu, F75252 Paris Cedex 05, France.*

Using Electromagnetically Induced Transparency (EIT) in a Cesium vapor, we demonstrate experimentally that the quantum state of a light beam can be mapped into the long lived Zeeman coherences of an atomic ground state. Two non-commuting variables carried by light are simultaneously stored and subsequently read-out, with no noise added. We compare the case where a tunable single sideband is stored independently of the other one to the case where the two symmetrical sidebands are stored using the same EIT transparency window.

PACS numbers: 03.67.- a, 03.65.Yz, 03.67.Hk, 42.50.Dv

Developing memory registers for quantum signals carried by light is an essential milestone for quantum information processing [1]. Atomic ensembles are good candidates for such registers since quantum states of light can be stored in long-lived atomic spin states and retrieved on demand. Several protocols have been proposed for such memories, based on three-level systems interacting with two light fields, in a Raman-type configuration [2, 3, 4] and in an electromagnetically induced transparency (EIT) configuration [5, 6, 7, 8], or based on a quantum non demolition (QND) interaction [9]. Substantial advances have been made in the single photon regime, including the storage of single photons [10, 11] and of entanglement [12] or the first demonstration of functional network following the DLCZ approach [13, 14, 15]. In the continuous variable regime, which is considered here, storage of non-commuting quantum variables of a light pulse has been demonstrated using the QND scheme [16]. Very recently, two experiments demonstrated the storage of a squeezed light pulse with partial retrieval of the squeezing [17, 18]. At present, while advances have been achieved in the direction of a quantum memory, it is interesting to investigate a variety of systems allowing more flexibility. In this paper, we study an EIT scheme allowing storage and retrieval of a single sideband quantum field on an adjustable frequency range, using atomic Zeeman coherence. The optimal response of the medium for storage can thus be adapted to the frequency to be stored by changing the magnetic field, while keeping the width of the EIT window rather narrow. If symmetrical sidebands are stored in separate atomic ensembles, this method should allow the storage of various quantum signals.

We consider a large ensemble of three-level atoms in a  $\Lambda$  level configuration interacting with two fields close to resonance with the atomic transitions. The protocol relies on a weak field carrying the quantum signal to be stored, and a strong, classical control field that makes the medium transparent by way of EIT for the signal field [19]. Due to the EIT process, the group velocity for the signal field is strongly reduced [20] and the signal pulse can even be stopped [21]. When the signal pulse is

entirely inside the atomic medium, it can be shown that the two quadratures of the field can be mapped into the transverse components of the ground state angular momentum. Models developed in Refs [5, 6, 7, 8] predict a high storage and retrieval efficiency. Moreover, taking into account all the noise sources, including the atomic noise generated by spontaneous emission and spin relaxation, a crucial result of the theoretical model developed in Ref. [7] is the absence of excess noise in the process of storage and retrieval, provided the optical depth of the medium is large enough.

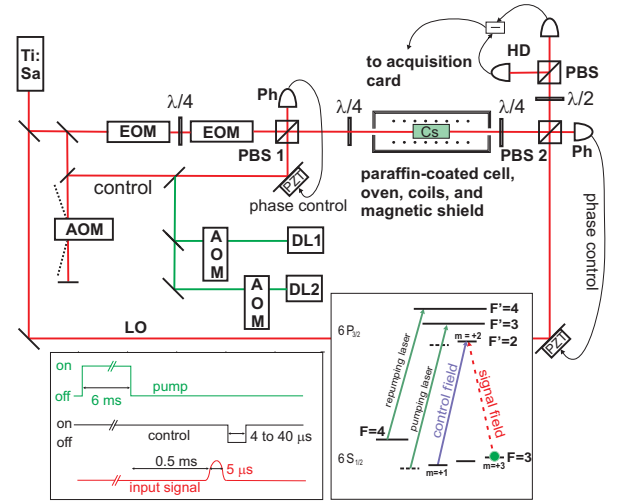


FIG. 1: Experimental set-up. DL 1 and 2 : pumping and repumping diode lasers. HD : homodyne detection. Ph : photodiode. EOM : electro-optical modulator. AOM : acousto-optical modulator. PBS : polarizing beam splitter. The control field intensity is controlled by an AOM, in double pass configuration in the zero<sup>th</sup> order (1:200 extinction). All laser beams have a  $1/e^2$  diameter of 14 mm in the cell. Insets : experimental sequence and Cs transitions involved.

The experimental scheme is based on cesium vapor in a magnetic field and uses the  $6S_{1/2}$ ,  $F=3$  to  $6P_{3/2}$ ,  $F'=2$  transition. The control beam is  $\sigma^+$  polarized and resonant with the  $m_F=1$  to  $m_{F'}=2$  transition while the signal field is  $\sigma^-$  polarized and resonant with the  $m_F=3$

to  $m_F=2$  transition (Fig. 1 inset). In order to fulfill the two-photon resonance condition, the detuning  $\Omega$  between the control and signal is equal to the Zeeman shift  $2\Omega_L$  between the two considered sub-levels. By tuning the magnetic field, one can optimize the memory response for a given frequency, allowing a widely tunable frequency range for the signal to be stored.

The experimental set-up is shown in Fig. 1. The cesium vapor is contained in a 3 cm long cell with a paraffin coating that suppresses ground state relaxation caused by collisions with the walls. The cell is heated to temperatures ranging from 30°C to 40°C, yielding optical depths from 6 to 18 on the signal transition. It is placed in a longitudinal magnetic field produced by symmetrical sets of coils and in a magnetic shield made of three layers of  $\mu$ metal. Residual magnetic fields are smaller than 0.2 mG, with a homogeneity better than 1:700. The atoms are optically pumped from the  $F=4$  to the  $F=3$  ground state and into the  $m_F = 3$  sublevel of the  $F=3$  ground state using diode lasers (2 mW and 0.2 mW respectively).

The control beam is produced by a stabilized Titanium-Sapphire (Ti:Sa) laser, with a linewidth of 100 kHz. The signal is a single sideband field frequency shifted from the laser frequency by a set of two electro-optical modulators. This sideband is a very weak coherent field, with a power on the order of a fraction of nanowatt, an adjustable frequency detuning  $\Omega$  and a polarization perpendicular to that of the carrier. The carrier is filtered out by a polarizing beamsplitter (PBS1 in Fig. 1) and used to lock the signal to control field relative phase. The light going out of the cell is mixed with a local oscillator and analyzed using a homodyne detection, after eliminating the control beam with a polarizing beamsplitter (PBS2 in Fig. 1). The local oscillator phase is locked to the one of the control beam after PBS2. In the experimental sequence, shown in Fig. 1 (inset), the atoms are first optically pumped for 6 ms into the  $m_F=3$  sublevel, with a 92% efficiency. After a dark period of 0.5 ms, a 1.6 to 5  $\mu$ s long signal pulse is sent into the cell for the writing procedure. The control field is then switched off for 4 to 40  $\mu$ s, and finally turned on again.

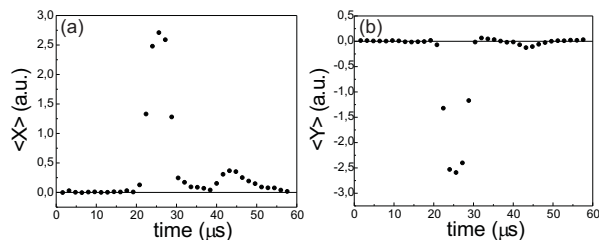


FIG. 2: Time-dependent mean values of the amplitude (a) and phase (b) quadratures, measured from a typical 2000-sequence run. Cell temperature  $T=40^\circ\text{C}$ , control field power = 10 mW, input pulse duration : 5  $\mu$ s, input intensity : 0.1 nW.

The photocurrent difference from the homodyne detec-

tion is recorded at a rate of  $50 \times 10^6$  samples per second with a 14-bit acquisition card (National Instruments NI 5122). A Fourier transform is performed numerically by multiplying the signal with a sine or a cosine function of frequency  $\Omega$  and integrating over a time  $t_m = n2\pi/\Omega$ , with  $n=2$  to 4. This yields sets of measured values of the quadrature operators  $\hat{X}$  and  $\hat{Y}$  of the outgoing field. Averaging over 2000 realizations of the experiment gives the quantum mean values  $\langle \hat{X} \rangle$  and  $\langle \hat{Y} \rangle$  and variances  $\langle (\Delta\hat{X})^2 \rangle = \langle (\hat{X})^2 \rangle - (\langle \hat{X} \rangle)^2$  and  $\langle (\Delta\hat{Y})^2 \rangle$  of the field quadratures. Typical traces for mean values are shown in Fig. 2, for a storage time of about 15  $\mu$ s. The first peak corresponds to the leakage of the signal field, the second one to the retrieved signal, for the in-phase ( $X$ ) quadrature (a) and for the out-of-phase ( $Y$ ) quadrature (b).

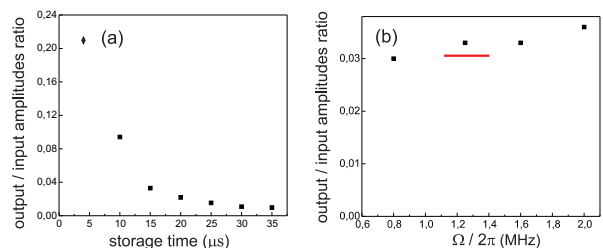


FIG. 3: (a) : Ratio of the amplitudes of the input and output states, as a function of the storage time.  $T=40^\circ\text{C}$ ; The points indicated by (■) (◆) correspond to a signal pulse duration of 6.4  $\mu$ s (1.6  $\mu$ s) with a control field power of 10 mW (140 mW). (b) : Ratio of the amplitudes of the input and output states, as a function of the modulation frequency  $\Omega/2\pi$ . The bar indicates the spectral width of the input pulse.

Let us first discuss the results on the mean values. The experiment clearly allows to store and retrieve the two quadratures of a signal in the atomic ensemble. The storage efficiency as a function of storage time is shown in Fig. 3 (a). It decreases rapidly with the storage time, with a time constant  $\tau_m \sim 10\mu\text{s}$ , due to fast spin decoherence processes in the ground state, which necessitates further investigation. An efficiency of 21% has been measured for a short storage time and a high value of the control field.

In order to check the coherence of the process, we have performed a detailed study of the phase of the retrieved signal [22]. Figure 4(a) shows the measured dependence of the phase  $\varphi_r$  of the retrieved pulse on the phase  $\varphi_i$  of the initial pulse. Phase  $\varphi_r$  has a linear dependence on  $\varphi_i$  with a unit slope, confirming the coherence of the process, while the non-zero value of  $\varphi_r$  for  $\varphi_i = 0$  corresponds to a phase shift accumulated by atomic coherence during the storage process. The latter is due to a non-zero detuning  $\delta = 2\Omega_L - \Omega \neq 0$  between the atomic coherence and the two-photon transition,  $\Omega_L$  being the Larmor frequency. In Fig. 4(b) we show the measured phase shift of the retrieved signal as a function of  $\delta$  by varying the magnetic

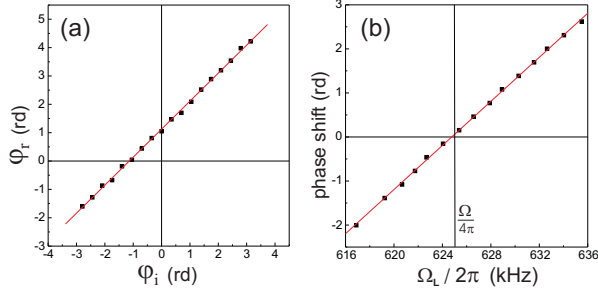


FIG. 4: Phase  $\varphi_r$  of the retrieved pulse (a) as a function of the input pulse phase  $\varphi_i$  with a constant  $\Omega_L$ , and (b) as a function of  $\Omega_L$ , with a fixed input phase. The storage time is  $20 \mu\text{s}$ , and  $\Omega/4\pi = 625 \text{ kHz}$

field for a fixed storage time. The phase shift has a linear dependence on the Larmor frequency, with a slope of  $0.25 \text{ rd/kHz}$  which is in very good agreement with the predicted dependence, given by  $\varphi_r = (2\Omega_L - \Omega)\tau$ , where  $\tau = 20 \mu\text{s}$  is the storage time.

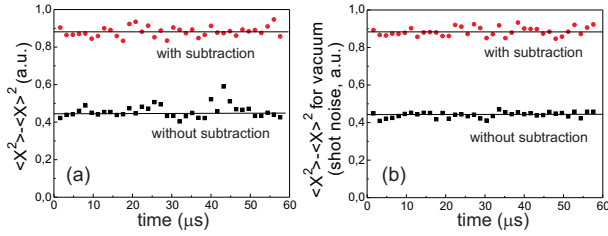


FIG. 5: (a) (resp. b) : variance of the amplitude quadrature for the signal (resp. for vacuum). The phase quadrature variance is similar.

The noise curves corresponding the mean values discussed above are obtained by calculating the variances from the same data set. Because of a small leak of the control field into the signal field channel, the raw data exhibit additional features due to the transients of the control field. Although it has been designed with a smooth shape, the control field contains Fourier components around  $\Omega/2\pi = 1.25 \text{ MHz}$ . To get rid of this spurious effect, the transients are measured independently after each sequence with no signal field and the corresponding data are subtracted point to point from the data taken with a signal field. The signal curves shown in Fig. 2 are obtained with this method. For the noise, this procedure is equivalent to a 50/50 beamsplitter on the analyzed beam and adds one unit of shot noise to the noise measured without subtraction, yielding the upper curve in Fig. 5(a). The noise calculated from the raw data, without subtraction, corresponding to the lower curve in Fig. 5(a), exhibits small additional fluctuations when the control field is turned on for read-out. With the subtraction procedure, these fluctuations are suppressed, showing that they originate from a classical, reproducible

spurious effect.

The noise curves can be compared to the shot noise, which is obtained independently from the same procedure with no control field and no signal field in the input, without and with subtraction, as shown in Fig. 5(b). The recorded variances shown in Fig. 5a are found to be at the same level as shot noise (Fig. 5b), which indicates that the writing and reading processes add very little noise, which can be evaluated to less than 2%. Excess noise has been studied by other authors [23, 25] and it is a critical feature for the storage benchmark. The noise curves of Fig. 5a correspond to moderate values of the control field power (10 mW). When the control field power is set to higher values, excess noise appears. It originates from fluorescence and coherent emission due the control beam [18] and from spurious fluctuations from the turn on of the control field leaking into the signal channel, that cannot be eliminated with the subtraction procedure.

Following Ref. [25], we can evaluate the performance of our storage device using criteria derived from the T-V characterization. This method had also been used to characterize quantum non demolition measurements or teleportation [26]. The conditional variance  $V$  of the signal field quadratures before and after storage is the geometrical mean value of the input-output conditional variances  $V = \sqrt{V_X V_Y}$  of the two quadratures, with  $V_X = V_X^{\text{out}} - \frac{|\langle \hat{X}^{\text{in}} \hat{X}^{\text{out}} \rangle|^2}{V_X^{\text{in}}}$  and the same for  $V_Y$ , where  $V_X^{\text{in/out}}$  is the variance of the normalized input/output field quadratures denoted  $\hat{X}^{\text{in/out}}$ . The transmission coefficient  $T$  is the sum of the transmission coefficients for the two quadratures  $T = T_X + T_Y$ , with  $T_X = \mathcal{R}_X^{\text{out}} / \mathcal{R}_X^{\text{in}}$ , where  $\mathcal{R}_X^{\text{in/out}}$  is the signal to noise ratio of input/output field for the  $X$  quadrature  $\mathcal{R}_X^{\text{in/out}} = \frac{4(\alpha_X^{\text{in/out}})^2}{V_X^{\text{in/out}}}$ , with  $\alpha_X^{\text{in/out}}$  the coherent amplitude of the fields.

The experimental results shown in Fig. 2 and 5, with a storage amplitude efficiency of 10%, corresponds to  $T = 0.02$  and  $V = 0.99$ , if one considers that the noise is equal to shot noise, and  $V = 1.01$  if the noise is 2% higher than shot noise. A classical memory with the same  $T$  yields  $V = 1.01$ . So, in this case, the performances of our system are within the limit of the quantum domain. When the storage amplitude efficiency is 21%, which is obtained with a smaller storage time and a higher control field,  $T = 0.08$ , while the value of the conditional variance of a system with such a  $T$  without excess noise is  $V = 0.96$  and the conditional variance for a classical memory is  $V = 1.04$ . The excess noise in our experiment in that case is over 10%, too large to reach the quantum domain.

The method presented here concentrates on the storage of a single sideband, which allows more flexibility than storing two symmetrical sidebands in the same EIT window, especially for high frequency components. We have measured the efficiency of the process when the sideband frequency  $\Omega$  is varied, as can be seen on Fig. 3 (b). No

significant variation with  $\Omega$  is observed. This comes from the fact that the frequency of the signal to be stored can be matched to the position of the EIT window, without changing its width. The EIT window width can be kept below 1 MHz, as shown in Fig. 6(a).

While many properties of quantum fields, such as squeezing, involve two symmetrical frequency sidebands, manipulation of individual sidebands provides an interesting tool for quantum information processing. The photocurrent difference after the homodyne detection, as measured here, yields the amplitude modulation operator  $\hat{X}(\Omega)$ ,

$$\hat{i} = \hat{X}(\Omega) = (\hat{X}_\Omega + \hat{X}_{-\Omega}) \cos \Omega t + (\hat{Y}_\Omega - \hat{Y}_{-\Omega}) \sin \Omega t \quad (1)$$

which is expressed as a combination of the quadrature operators of the two sidebands,  $\hat{X}_{\pm\Omega}$  and  $\hat{Y}_{\pm\Omega}$ . In our present case, with a single sideband, the observables to be measured,  $\hat{X}_\Omega$  and  $\hat{Y}_\Omega$ , are mixed with an empty sideband at  $-\Omega$ , adding one unit of shot noise, which is intrinsic to homodyne detection. In the case of a squeezed field, we have  $\Delta^2 \hat{X}(\Omega) < 1$  and Eq. 1 shows that the two sidebands are entangled, as known for a long time [24].

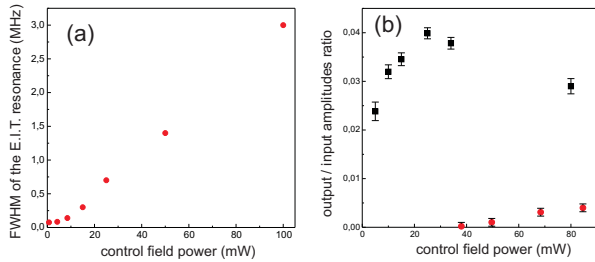


FIG. 6: (a) FWHM of the EIT transparency window (MHz) as a function of the control field power (mW). The control and signal beams waist is 7.2 mm. (b) ratio of the output and input states amplitudes, as a function of the control field power, for a single sideband of frequency 1.25 MHz (squares) and a dual sideband modulation of frequency 400 kHz (circles).  $T = 50^\circ\text{C}$ . Pulse duration : 5  $\mu\text{s}$ . Storage time : 15  $\mu\text{s}$ .

To store a squeezed field at a given frequency  $\Omega$ , one has to store its two entangled sidebands at  $+\Omega$  and  $-\Omega$ , which can be achieved by extending our method, first separating the two sidebands using a Mach-Zehnder interferometer [27] and storing them into two atomic ensembles. The procedure results in entangling the two ensembles. After read-out, the two sidebands can eventually be recombined and measured with no vacuum added.

The two sidebands of a field can also be stored at the same time in one atomic ensemble if  $2\Omega$  is smaller than the width of the EIT transparency window. Figure 6(a) shows the EIT linewidth in our case as a function of the control field power. We have measured the efficiency of the storage process for a signal field made of two sidebands at  $\pm 400$  kHz. The result is shown in Fig. 6(b). The efficiency is lower than in the single sideband case,

which can be attributed to the large value of the time-bandwidth product of the pulse to be stored.

In conclusion, we have demonstrated storage and retrieval of the two non-commuting quadratures of a small coherent state in an atomic medium, with an excess noise small enough to put it inside the quantum domain. This coherent state, made of a single sideband of the control field, has been stored in the Zeeman coherence of the atoms. Tuning the magnetic field allows to adjust the response of the medium to the signal frequency, keeping the EIT window rather narrow. Comparison with the storage of a modulation made of two symmetrical sidebands shows the latter is hampered by the finite bandwidth of the EIT window. Storing the two sidebands in two separate atomic ensembles is thus a promising method for quantum memory with a widely adjustable frequency. The method also opens the way to the storage of multiplexed quantum signals, a promising direction to increase the capacity of a quantum network.

The authors thank Xiao Jun Jia for valuable contributions. This work was supported by the E. U. grants COVAQIAL and COMPAS, by the French ANR contract IRCOQ and by the Ile-de-France programme IFRAF.

\* email : elg@spectro.jussieu.fr

- 
- [1] P. Zoller *et al.*, Eur. Phys. J. D **36**, 203 (2005).
  - [2] A.E. Kozhekin *et al.*, Phys. Rev. A **62**, 033809 (2000).
  - [3] L.M. Duan *et al.*, Nature (London) **414**, 413 (2001).
  - [4] A. Dantan *et al.*, Phys. Rev. A **67**, 045801 (2003).
  - [5] M.D. Lukin *et al.*, Phys. Rev. Lett. **84**, 4232 (2000).
  - [6] M. Fleischauer and M.D. Lukin, Phys. Rev. Lett. **84**, 5094 (2000).
  - [7] A. Dantan and M. Pinard, Phys. Rev. A **69**, 043810 (2004).
  - [8] A. Dantan *et al.*, Phys. Rev. A **73**, 032338 (2006).
  - [9] K. Hammerer *et al.*, Phys. Rev. A **70**, 044304 (2004).
  - [10] M.D. Eisaman *et al.*, Nature **438**, 837 (2005).
  - [11] T. Chanelire *et al.*, Nature **452**, 67 (2008).
  - [12] K. S. Choi *et al.*, Nature **438**, 828 (2005).
  - [13] C. W. Chou *et al.*, Nature **438**, 828 (2005); J. Laurat *et al.*, Optics Express **14**, 6912 (2006); C. W. Chou *et al.*, Science **316**, 1316 (2007).
  - [14] S. Chen *et al.*, Phys. Rev. Lett. **97**, 173004 (2006).
  - [15] J.K. Thompson *et al.*, Science **313**, 74 (2006).
  - [16] B. Julsgaard *et al.*, Nature **432**, 482 (2004).
  - [17] K. Honda *et al.*, Phys. Rev. Lett. **100**, 093601 (2008).
  - [18] J. Appel *et al.*, Phys. Rev. Lett. **100**, 093602 (2008).
  - [19] S.E. Harris *et al.*, Phys. Rev. Lett. **64**, 1107 (1990).
  - [20] L.V. Hau *et al.*, Phys. Rev. Lett. **82**, 4611 (1999).
  - [21] C. Liu *et al.*, Nature (London) **409**, 490 (2001); D.F. Phillips *et al.*, Phys. Rev. Lett. **86**, 783 (2001).
  - [22] A. Mair *et al.*, Phys. Rev. A **65**, 031802(R), (2002).
  - [23] M.T.L. Hsu *et al.*, Phys. Rev. Lett. **97**, 183601 (2006).
  - [24] C.M. Caves, Phys. Rev. D **26**, 1817, (1982); J. Gea-Banacloche and G. Leuchs, J. Mod. Opt. **34**, 793 (1987).
  - [25] G. Hetet *et al.*, Phys. Rev. A **77** 012323 (2008).
  - [26] J.F. Roch *et al.* Phys. Rev. Lett. **78** 634 (1997); T.C.

- Ralph and P.K. Lam, Phys. Rev. Lett. **81** 5668 (1998).  
[27] O. Glöckl *et al.*, Opt. Lett. **29**, 1936 (2004).